Supporting Information for

Ag/AgCl Clusters Derived from AgCu Alloy Nanoparticles as Electrocatalyst for Oxygen Reduction Reaction

Timuçin Balkan[1,2,3], Hüseyin Küçükkeçeci[2], Dilan Aksoy[1,2], Messaoud Harfouche[4], Önder Metin[1,2,5], Sarp Kaya[1,2,5,*]

[1]*Koç University Tüpraş Energy Center (KUTEM), 34450 Sarıyer, Istanbul, Turkey*

[2]*Department of Chemistry, Koç University, 34450 Sarıyer, Istanbul, Turkey*

[3]*n²STAR Koç University Nanofabrication and Nanocharacterization Center for Scientific and Technological Advanced Research, 34450 Sarıyer, Istanbul, Turkey*

[4]*Synchrotron-light for Experimental Science and Applications in the Middle East (SESAME), Allan 19252, Jordan*

[5]*Koç University Surface Science and Technology Center (KUYTAM), 34450 Sarıyer, Istanbul, Turkey*

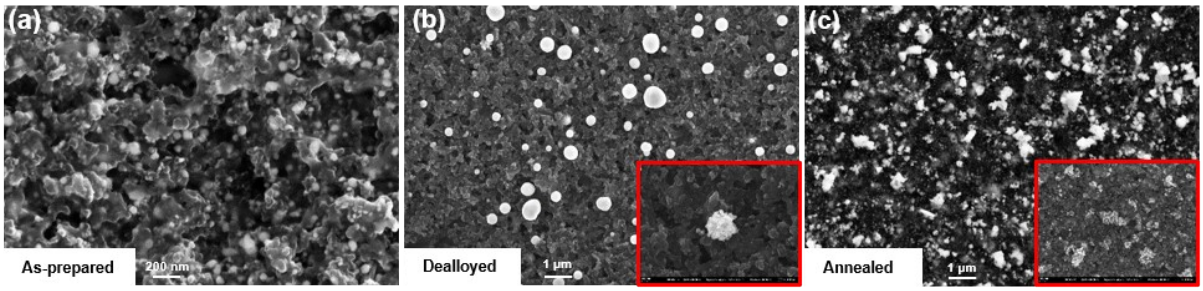

Figure S1. FESEM images of (a) as-prepared, (b) dealloyed, and (c) annealed Ag_7Cu_3 alloy NPs.

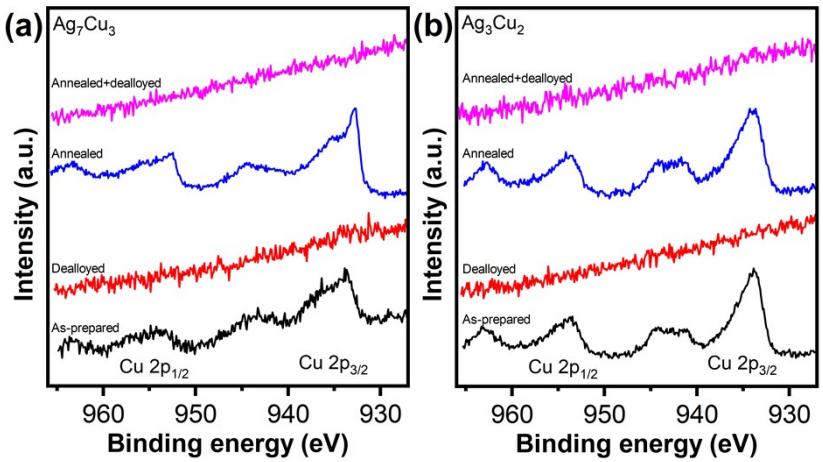

Figure S2. Cu 2p spectra of (a) Ag_7Cu_3 and (b) Ag_3Cu_2.

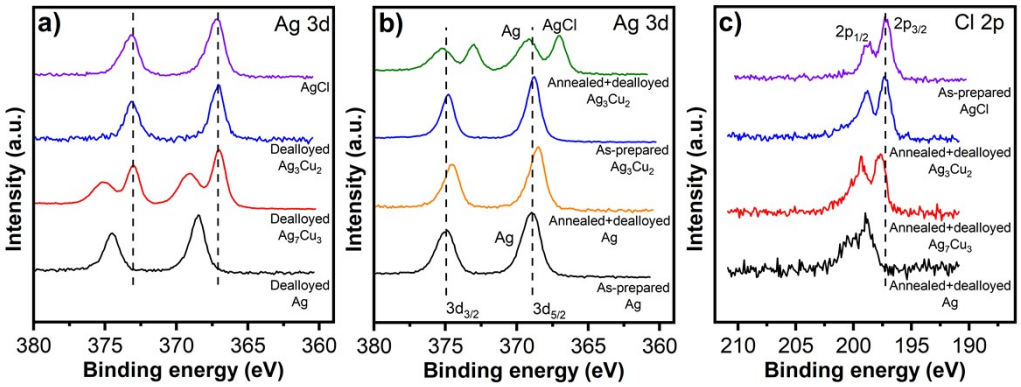

Figure S3. (a-b) Ag 3d and (c) Cl 2p XPS spectral changes upon annealing and dealloying.

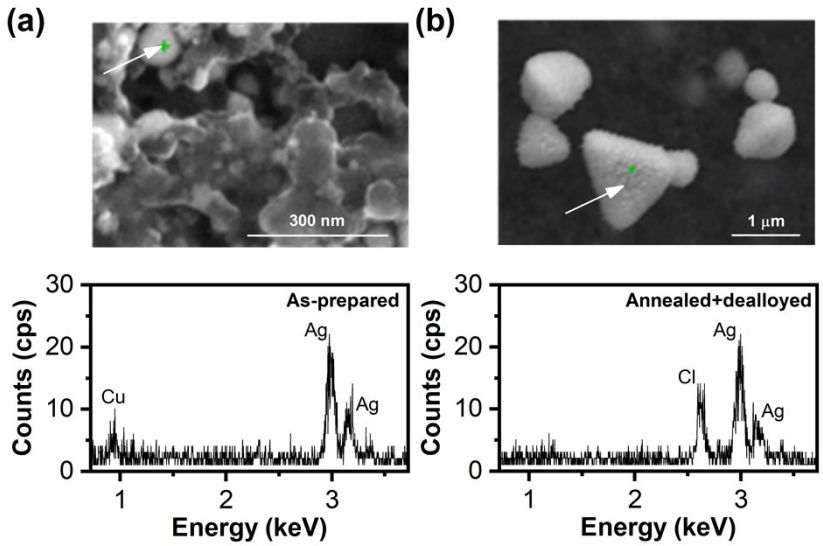

Figure S4. EDS analysis of (a) as-prepared and (b) annealed+dealloyed Ag_7Cu_3 NPs.

Table S1: Structural parameters around Ag derived from EXAFS data fitting

Ag_7Cu_3	Bond	N (atoms)	R (Å)	σ_2 (Å^2)
Dealloyed+annealed	Ag-Cl	0.12±0.1	1.70±0.002	0.001±0.0001
	Ag-Ag	8.36±0.4	2.74±0.001	0.0025±0.0003*
	Ag-Ag	3.20±0.6	4.18±0.005	0.0025±0.0003*

* parameters correlated

Note: The number of atoms is relative and under-estimated because of the significantly high noise at higher k.

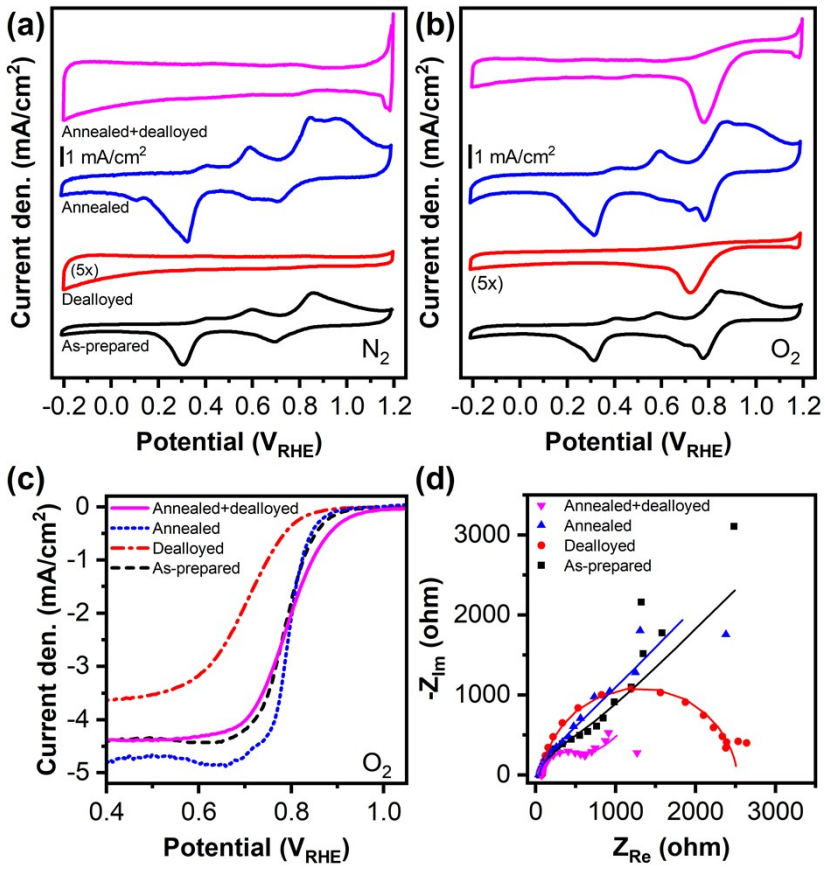

Figure S5. CV curves of Ag_3Cu_2 NPs in (a) N_2 saturated and (b) O_2 saturated 0.1 M KOH. (c) RDE polarization curves of AgCu NPs at 1200 rpm in O_2 saturated 0.1 M KOH. d) Nyquist plots recorded in O_2 saturated 0.1 M KOH under bias (0.83 V_{RHE}). Solid lines represent fitting performed by adopting the equivalent circuit model.

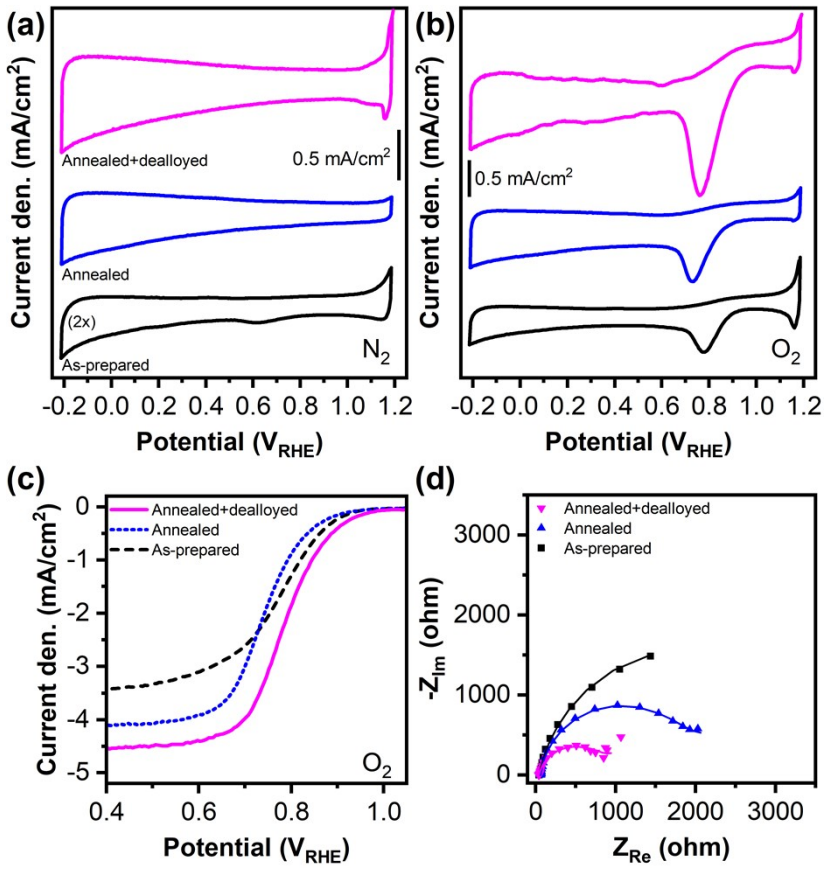

Figure S6. CV curves of Ag NPs in (a) N_2 saturated and (b) O_2 saturated 0.1 M KOH. (c) RDE polarization curves of Ag NPs at 1200 rpm in O_2 saturated 0.1 M KOH. (d) Nyquist plots recorded in O_2 saturated 0.1 M KOH under bias (0.83 V_{RHE}). Solid lines represent fitting performed by adopting the equivalent circuit model.

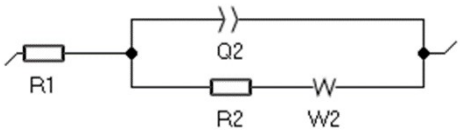

Figure S7. The equivalent circuit model adopted to determine solution resistance R_s (from R1), charge transfer resistance R_{ct} (from R2), and Warburg resistanceW (from W2).

Table S2. Equivalent circuit modeling data of Ag_7Cu_3 NPs.

Circuit Elements	As-prepared	Dealloyed	Annealed	Annealed+dealloyed
R1 (ohm)	80.6±0.2	72.6±0.2	57±0.2	43.7±0.2
R2 (R_{ct}) (ohm)	699.9±1.2	3335±0.4	549.8±14.8	425.4±2.5
Q2 ($F.s^{(a-1)}$)	$0.4\times10^{-3}\pm2.8\times10^{-6}$	$0.2\times10^{-3}\pm0.1\times10^{-6}$	$0.8\times10^{-3}\pm13.3\times10^{-6}$	$1\times10^{-3}\pm11.8\times10^{-6}$
a2	0.9±0.5	0.9±0.5	0.9±0.5	1±0.5
W2 ($ohm.s^{-1/2}$)	174.6±0.5	-	430.6±0.6	198.3±0.7

Table S3. Equivalent circuit modeling data of Ag_3Cu_2 NPs.

Circuit Elements	As-prepared	Dealloyed	Annealed	Annealed+dealloyed
R1 (ohm)	56.7±0.2	78±0.2	48±0.2	76.8±0.2
R2 (R_{ct}) (ohm)	602.3±15.7	2445±0.4	447.4±37	530.2±1.5
Q2 ($F.s^{(a-1)}$)	$0.4\times10^{-3}\pm8.8\times10^{-6}$	$0.2\times10^{-3}\pm0.2\times10^{-6}$	$1.0\times10^{-3}\pm31.7\times10^{-6}$	$0.7\times10^{-3}\pm5.7\times10^{-6}$
a2	0.9±0.5	0.9±0.5	0.9±0.5	0.9±0.5
W2 ($ohm.s^{-1/2}$)	589.1±1.4	-	497.7±2.7	114.9±0.6

Table S4. Equivalent circuit modeling data of Ag NPs.

Circuit Elements	As-prepared	Annealed	Annealed+dealloyed
R1 (ohm)	47.7±0.2	64.4±0.2	44.1±0.2
R2 (R_{ct}) (ohm)	3789±10.5	1839±7.4	802±6.9
Q2 ($F.s^{(a-1)}$)	$0.6\times10^{-3}\pm2\times10^{-6}$	$0.8\times10^{-3}\pm1.4\times10^{-6}$	$1.1\times10^{-3}\pm3.5\times10^{-6}$
a2	0.9±0.5	0.9±0.5	0.9±0.5
W2 ($ohm.s^{-1/2}$)	-	73.48±1	52.7±1.2

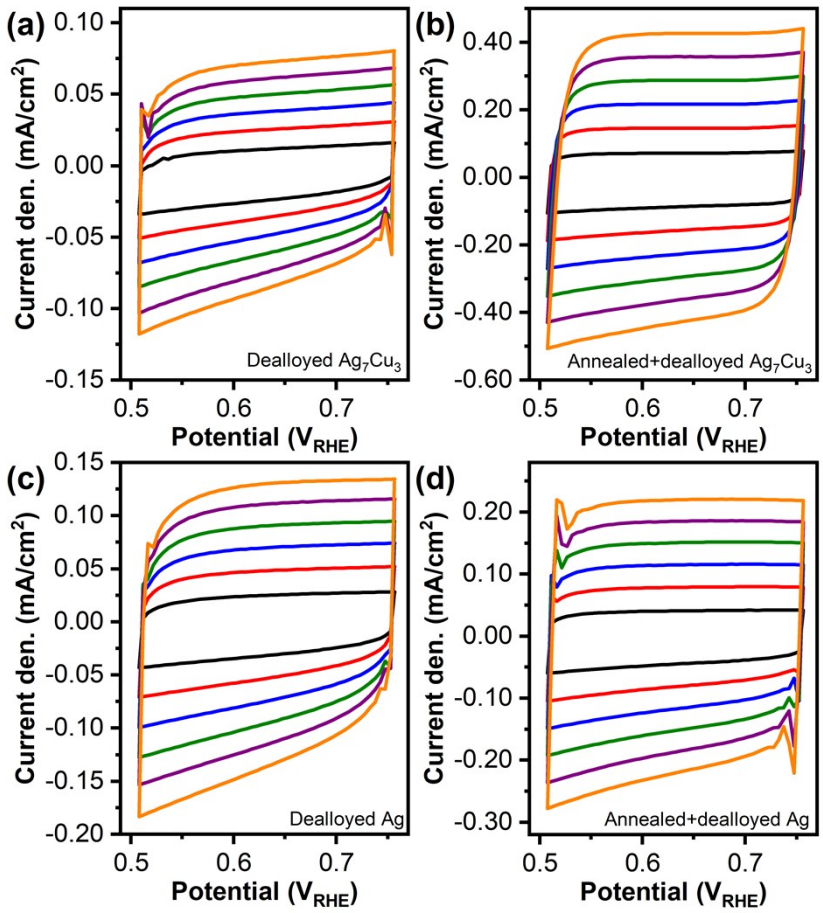

Figure S8. (a-d) CV curves of dealloyed and dealloyed+annealed Ag_7Cu_3 and Ag with scan rates from 10 mV/s to 60 mV/s.

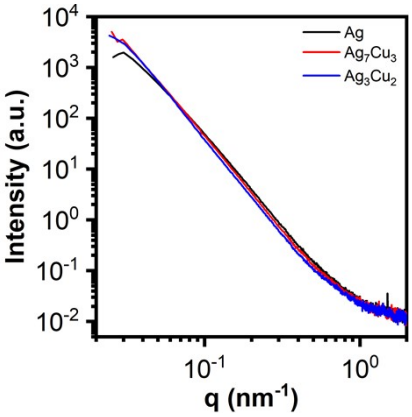

Figure S9. SAXS pattern of dealloyed+annealed Ag, Ag_7Cu_3, and Ag_3Cu_2 NPs.

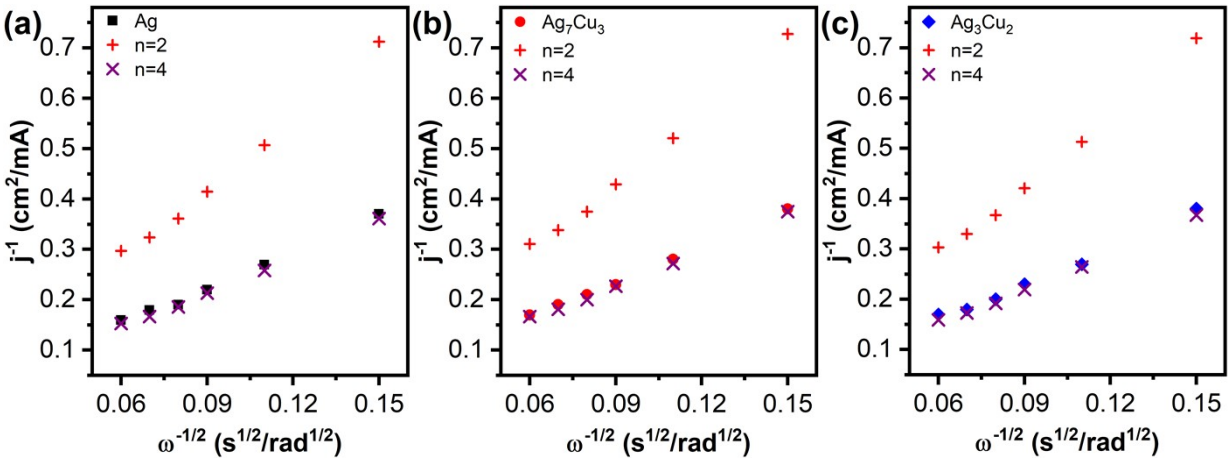

Figure S10. Koutecky-Levich plots for (a) Ag, (b) Ag_7Cu_3, and (c) Ag_3Cu_2 extracted from RDE polarization curves at 0.5 V_{RHE}. Experimental data represents electrocatalysts after annealing+dealloying treatment and were compared with the theoretical calculations assuming 2 and 4 electron transfer processes.

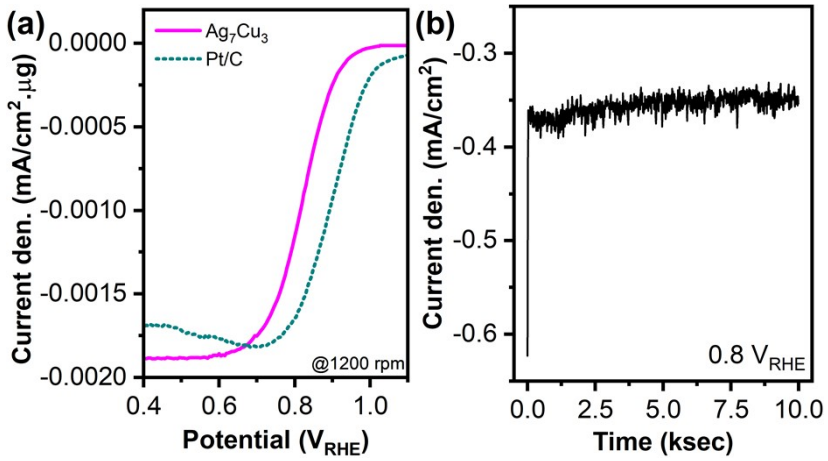

Figure S11. (a) Comparison of RDE curves of annealed+dealloyed Ag_7Cu_3 NPs and commercial Pt/C. Stability test of annealed+dealloyed Ag_7Cu_3 under constant potential in O_2 saturated 0.1 M KOH.

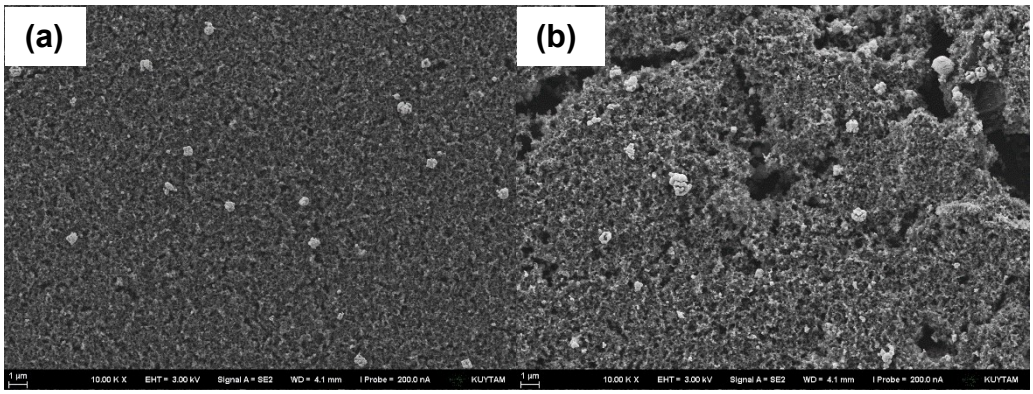

Figure S12. SEM images of annealed+dealloyed Ag_7Cu_3 (a) before and (b) after electrochemical test at 0.8V vs. RHE for 3 hours.

Table S5. Selected onset and half-wave potentials from the literature.

Sample	E_{onset} (V_{RHE})	$E_{1/2}$ (V_{RHE})	Study
Ag_9Pd_1 Alloy	1.02	0.89	[1]
Ag@N-C	0.96	0.82	[2]
$Ag@Ag_2WO_4$	0.89	0.66	[3]
Ag/ZrO_2/MWCNT	0.97	0.79	[4]
CuAg@Ag/N-GNS	0.94	0.85	[5]
Fe-NC	0.96	0.88	[6]
Ann.+Dea. Ag_7Cu_3	0.97	0.83	This work

References

1 X. Qiu, X. Yan, K. Cen, H. Zhang, G. Gao, L. Wu, D. Sun and Y. Tang, *Journal of Energy Chemistry*, 2019, **28**, 111–117.
2 L. Zhang, X. Wang, T. Zhang, C. Liu, D. Li and S. Xing, *Journal of Alloys and Compounds*, 2019, **785**, 491–498.
3 K. Nubla and N. Sandhyarani, *Electrochimica Acta*, 2020, **340**, 135942.
4 A. Meng, L. Lin, X. Yuan, T. Shen, Z. Li and Q. Li, *ChemCatChem*, 2019, **11**, 2900–2908.
5 T. D. Thanh, N. D. Chuong, H. V. Hien, N. H. Kim and J. H. Lee, *ACS Appl. Mater. Interfaces*, 2018, **10**, 4672–4681.
6 Y. Wang, Y. Pan, L. Zhu, H. Yu, B. Duan, R. Wang, Z. Zhang and S. Qiu, *Carbon*, 2019, **146**, 671–679.